Evolution of electrical resistivity and NMR during early-stage maturation of an organic-rich chalk

Eva G. Vinegar[1,*], *Yoav O.* Rosenberg[2], *Scott V.* Nguyen[3] , *Larry W.* Lake[1], and *Harold J.* Vinegar[4]

[1]The University of Texas at Austin
[2]Geological Survey of Israel
[3]17TeraWatts
[4]Vinegar Technologies, LLC

Abstract. This paper studies the changes in the electrical resistivity of an organic-rich source rock chalk containing a Type-IIs kerogen during early-stage maturation of the kerogen. As bitumen is generated during maturation, the chalk changes from water wet to a complex mixed-wet pore system, with the micritic pore space remaining water wet while the bitumen expelled into the macro pores converts some pores to oil wet. This mixed-wet system results in non-Archie electrical behavior with pronounced curvature of the I-S_w curve. We find that this curvature is well fit by connectivity theory. The connectivity theory parameters are determined both on native state core and from artificial laboratory pyrolysis which generates bitumen. NMR is used to distinguish the brine in micritic, water-wet pore spaces from that in the intergranular, mixed-wet pore spaces, from which the observed connectivity parameters may be independently estimated. Comparison between electrical resistivity and dielectric logs show that the connectivity parameters match the laboratory results over a calcareous section more than 300 m thick.

Introduction

The Late Cretaceous Ghareb-Mishash formation in Israel provides a unique opportunity to study the evolution of electrical resistivity and NMR responses to organic maturation in a source rock chalk. This chalk has an extremely high TOC up to 15 wt%. In the coastal plain containing the Shefela basin, the organic-rich chalk has experienced shallow burial and the kerogen is immature. In contrast, in the Golan basin in northern Israel, the same Ghareb-Mishash formation has been buried much deeper and experienced a higher geothermal gradient, leading to a higher level of kerogen maturation to bitumen. Using core and log data from both basins, we have been able to follow the change in the electrical resistivity and NMR responses from immature to early-stage organic maturation.

The early-stage mature, kerogen-rich Late Cretaceous formation in the Golan basin is characterized by large amounts of bitumen and light hydrocarbons which affect the connectivity of the fluids within the rock and thus the electrical resistivity and NMR responses. Increasing burial of these organic-rich chalks affects connectivity by compaction (reduction in porosity) and by organic maturation of the kerogen (hydrocarbon generation and wettability changes).

Electrical resistivity, dielectric and NMR data are used to aid the interpretation of petrophysical properties of reservoir rocks, such as porosity, pore size, fluid type, fluid saturation, tortuosity, and permeability [1, 2]. Improvements to the models and interpretations used to evaluate the petrophysical properties have been ongoing with the development of unconventional resource plays. For example, extremely high values of electrical resistivity are common in mixed-wet micritic calcites and are difficult to model using Archie's resistivity model which is applicable to conventional reservoir rocks. Cementation and saturation exponents are about 2 for conventional rocks, but often vary significantly for vuggy rocks, shaly sands, and mixed or oil-wet systems. Furthermore, the Archie exponents selected may not fit well for a range of water saturations. Several resistivity models have been developed to better fit the electrical resistivity in different types of rock systems, but few fit the curvature of the resistivity index with water saturation [3-6]. A more general form of Archie's resistivity model based on connectivity theory provides a more consistent fit with relatively few parameters [5,6].

In agreement with connectivity theory, the electrical resistivity in the Ghareb-Mishash formations shows a sharp increase in I-Sw curvature for early-stage thermal maturation. The change from Archie-type behavior in the Shefela basin to I-Sw curvature in the Golan basin is due to the generation and expulsion of bitumen from the kerogen, which blocks many of the pore throats in the dual-porosity system and creates mixed wet or oil-wet surfaces in the larger, intergranular pore spaces.

* Corresponding author: evavinegar@gmail.com

We first present a brief review of connectivity theory. We then show how the resistivity index changes from Archie-type behavior to non-Archie behavior once the organic-rich chalk is artificially matured. We show how bitumen content increases with depth and maturation in the Ghareb basin. As bitumen is generated during maturation, the chalk changes from water wet to a complex mixed-wet pore system, with the micritic pore space remaining water wet while the bitumen expelled into the macro pores converts some pores to oil wet. This mixed-wet system results in non-Archie electrical behavior with pronounced curvature of the I-S_w. We show that this curvature is well fit by connectivity theory. The connectivity theory parameters are then determined on native state core and found to match those found during artificial laboratory pyrolysis. NMR is used to distinguish the brine in micritic, water-wet pore spaces from that in the intergranular, mixed-wet pore spaces, from which the observed connectivity parameters may be independently estimated. Finally, we compare electrical resistivity and dielectric logs and show that the connectivity parameters match the laboratory results over a 350 m calcareous section.

Electrical resistivity and connectivity theory

The petroleum industry has long used Archie's equation [7] to estimate the hydrocarbon saturation of reservoirs using resistivity and porosity logs. Archie's equation is:

$$R_t = \frac{R_w}{\phi^m S_w^n} \quad (1)$$

where R_t is the total resistivity of the rock, R_w is the resistivity of the brine, ϕ is the porosity, S_w is the water saturation, m is the cementation exponent, and n is the saturation exponent.

The sensitivity of oil reserve estimates to the value of these exponents has been critical for reservoir evaluation and project decisions. For many reservoirs, m is about 2, but can be much higher for vuggy rocks. n is usually about 2 in clean, water-wet sandstones, less than 2 in shaly sands, and much more than 2 in mixed-wet and oil-wet systems. Heterogeneous systems further make it difficult to fit these exponents to a dataset.

Deviation from the Archie straight line values on a resistivity index versus water saturation log-log plot is a common issue in assessing many reservoir rocks. The Archie saturation exponent needed to match data on this plot changes significantly with water saturation [6, 8]. Several methods were developed to represent the saturation in non-Archie rocks. Montaron [5,6] proposed a more generalized version of Archie's equation based on percolation theory:

$$R_t = R_w \left[\frac{1-P_c}{P-P_c}\right]^{\mu} \quad (2)$$

where R_t is the electrical resistivity of the system, R_w is the electrical resistivity of the conductive portion, P is the probability that a portion of the rock will be conductive (water volume fraction), Pc is the percolation threshold (Montaron calls P_c a water connectivity correction index, χ_w), and μ is the conductivity exponent (~2). The water volume fraction is the water saturation times the porosity of the rock, $S_w\varphi$, giving:

$$R_t = R_w \left[\frac{1-\chi_w}{S_w\phi-\chi_w}\right]^{\mu} \quad (3)$$

This connectivity equation elegantly accounts for the curvature of the resistivity index with saturation in some systems. We note that when the percolation threshold is 0, the connectivity equation reduces to Archie's equation if m=n. Montaron further derived this connectivity equation for a variety of cases using a modified CRIM mixing law [9,10]. We find this particularly applicable to the organic-rich Ghareb-Mishash chalk.

As described in Vinegar et al. [11], **Fig. 1** shows a core sample from the Shefela containing immature organic matter that was artificially matured and its resistivity index versus brine saturation. T_{max} is 421°C for the post-pyrolysis sample and the porosity is 50 pu. The blue circles represent measurements taken post-pyrolysis (dry pyrolysis), and the red circles represent measurements taken pre-pyrolysis. An Archie equation fits the pre-pyrolysis data with a saturation exponent n=1.93. The model based on connectivity theory fits the post-pyrolysis data with $\chi_w = 0.03$ and $\mu = 2$. The results show curvature beginning to develop at lower values of water saturation.

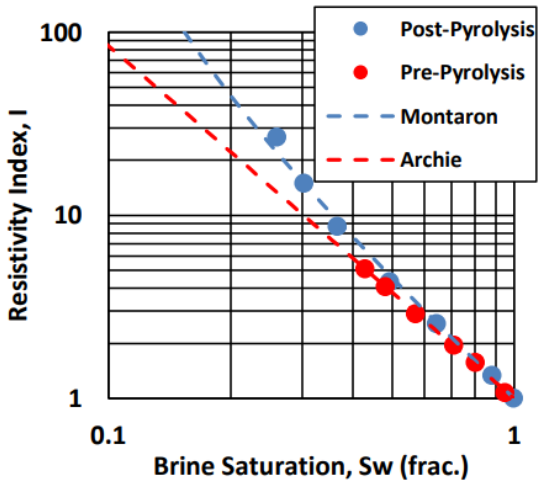

Fig. 1: Resistivity index versus brine saturation for an immature core sample from the Shefela basin pre- and post-pyrolysis [11].

We can show the deviation of the electrical resistivity from Archie's equation using connectivity theory [6]. The water connectivity correction index primarily controls the curvature of the resistivity index versus water saturation plot. There are two main contributors to the water connectivity correction index: one due to the micritic pore space and one due to the oil-wet pore space.

The water-filled pores of the micritic space are highly connected, and the conductivity exponent of micritic grains is often taken to be 1.5 as a result (as Montaron points out, 1.5 is the conductivity exponent for

a packing of spherical grains). If the micritic space contributes to the electrical resistivity, then the electrical resistivity would be slightly less resistive than if one were to consider only larger, intergranular pore spaces. A non-organic, water-wet carbonate containing a dual micro and meso-macropore system would consist of three phases: micritic grains, water in the intergranular pore space, and solid grains. The micritic grains are treated as an independent unit with its micropores Montaron [5,6] derived the equation for the water connectivity correction index for a rock containing micritic grains:

$$\chi_w = x_m\left(\phi_m - \phi_m^{\mu_m/\mu}\right) \quad (4)$$

where χ_w is the water connectivity correction index, x_m is the volume fraction of the rock containing micritic grains, ϕ_m is the porosity of the micritic portion of the rock, μ_m is the conductivity exponent of the micritic portion of the rock, and μ is the conductivity exponent of the intergranular portion of the rock.

Assuming that x_m is around 0.25, μ_m is 1.5, and μ is 2, χ_w can be strongly negative, as shown in **Fig. 2a**. Negative values of χ_w suggest that compared to Archie, the resistivity index would be much smaller, especially with decreasing water saturation. If the system is fully water-saturated, however, in many cases the resistivity index will be close to that predicted by Archie.

If we neglect the micritic space and consider a system where the larger pore spaces are mixed-wet, with some water-wet pores and some oil-wet pores, then the water connectivity correction index as derived by Montaron [6] is:

$$\chi_w = x_o S_{co} \phi_M \quad (5)$$

where x_o is the fraction of pores that are oil-wet, S_{co} is the critical oil saturation at which the conductive fluids no longer percolate, and ϕ_M is the porosity of the macro pores. χ_w is positive and grows linearly.

In the early-stage mature case, where the bitumen has partially blocked the pore throats of the micritic space, $\chi_w = x_o S_{co} \phi_M$ is positive and the resistivity index compared to Archie is higher, especially with decreasing water saturation.

For the case in which there are oil-wet spaces and there is connectivity between the brine in the micritic space and that in the larger pore spaces, χ_w is the sum of the two terms:

$$\chi_w = x_m\left(\phi_m - \phi_m^{\frac{\mu_m}{\mu}}\right) + x_o S_{co} \phi_M \quad (6)$$

where the first term is negative, and the second term is positive.

Fig. 2a shows the behavior of χ_w with x_m and ϕ_m due to the micritic grains. Over a large range of porosities inside the micritic portion of the rock, χ_w does not vary significantly, particularly if the bulk volume fraction of micritic grains is low. **Fig. 2b** shows the behavior of χ_w due to the oil-wet pore spaces. With burial and compaction, the porosity of the oil-wet pore spaces decreases, but the oil-wet fraction of the intergranular pore spaces increases. These factors keep χ_w more stable along the length of the organic-rich portion of the well.

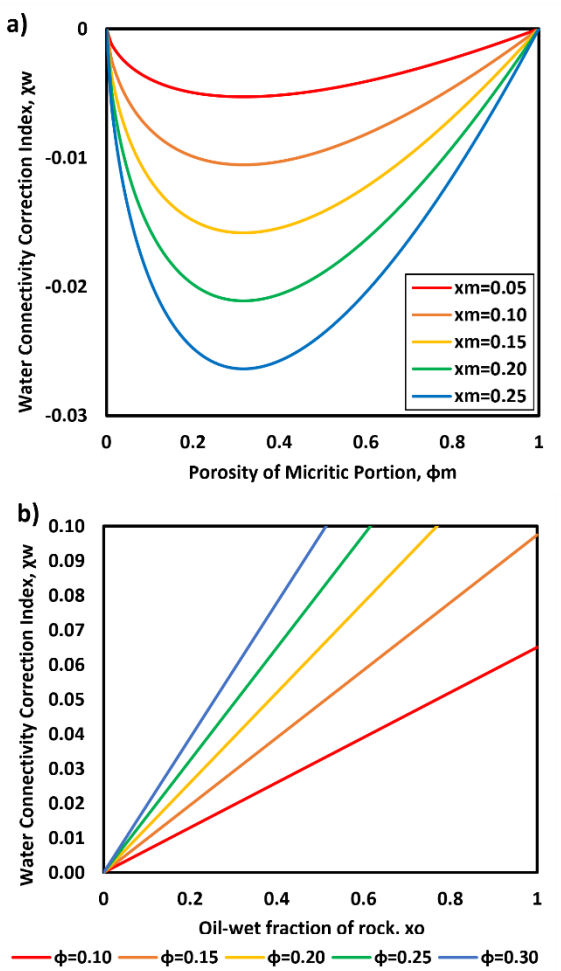

Fig. 2*:* **a)** χ_w for a micritic portion of the rock in which μ_m is 1.5 and μ is 2 in equation (4). **b)** χ_w for a rock with oil-wet pore spaces in which S_{co} is 0.65 in equation (5). ϕ is the porosity of the macro pore space.

Creating Oil-Wet Spaces with Bitumen Generation

The immature organic-rich chalk from the Shefela basin is water wet. In contrast, the early-stage mature kerogen from the Golan basin has generated bitumen and light hydrocarbons, and thus created oil-wet surfaces. These oil-wet surfaces induce the curvature in the resistivity index. Furthermore, the distribution of the organic matter in the rock cause much of the micritic water-wet pore spaces to be blocked by bitumen.

The SEM images in **Fig. 3** from Vinegar et al. [11] show the distribution of the pore spaces and organic matter. The upper right image is the base SEM image. The circular coccoliths and larger calcite grains are shown in the upper right image in green (calcium mapping using SEM-EDS). The lower left image shows the kerogenous organic matter dispersed between the larger calcite grains. Sulfur mapping was used to identify the organic matter because Type II-s kerogen (S/C ratio above 0.04) is dominant in this rock [12]. The lower right image shows the pore spaces, organic matter, and calcite. The co-deposition of organic matter and calcite minerals allow for bitumen generation to enter the macropore system and

block many of the entrances to the micritic pore space. This observation agrees with the change in NMR diffusional coupling from strong to weak as the kerogen generates bitumen [2,11].

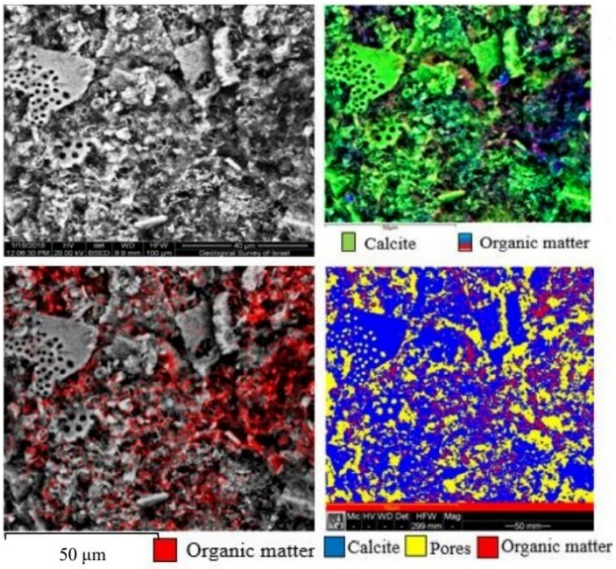

Fig. 3: SEM (upper left) and SEM-EDS images showing calcite, organic matter, and pores for the organic-rich chalk [11].

An immature, organic-rich Ghareb rock was artificially matured in a semi-open pyrolysis reactor gradient experiment [13]. The sample was evaluated in a Vinci Technologies Rock-Eval 6 analyzer to determine T_{max} and hydrocarbon content with TOC. Bitumen was obtained from cuttings using a Soxhlet extractor (Vinci Technologies) with dichloromethane and methanol solvent (9:1 V/V). **Fig. 4** shows the bitumen and light hydrocarbon content versus T_{max} and the corresponding windows of hydrocarbon generation. Bitumen generation begins at a T_{max} value of about 417°C.

Fig. 5 shows the bitumen content (wt%) with depth for the NESS 2 well in the Golan basin. There is significant bitumen content over the 350 meters. This is quite different from the immature organic-rich rock from the Shefela basin, where there is very low bitumen content. The porosity decreases from the upper to lower portion of the well.

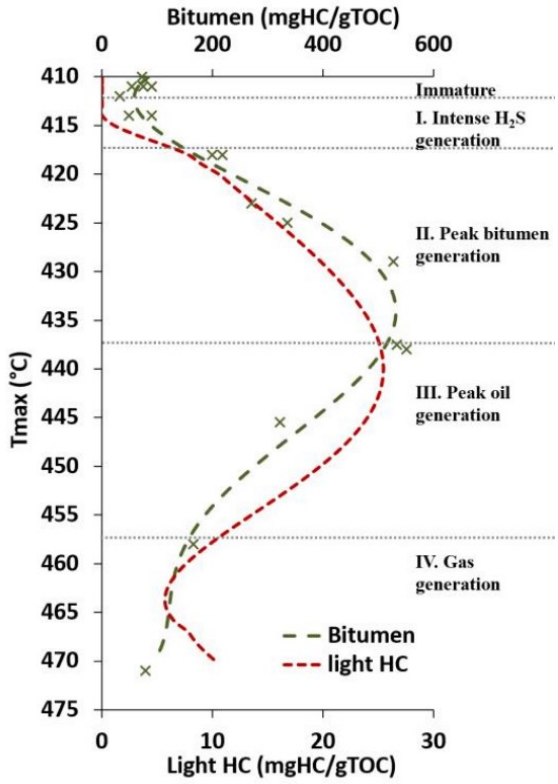

Fig 4: Bitumen and light hydrocarbon generation versus T_{max} of an artificially matured organic-rich Ghareb sample from the Shefela basin. The immature stage, hydrogen sulfide, bitumen, oil, and gas windows are marked by the dotted lines [11,13].

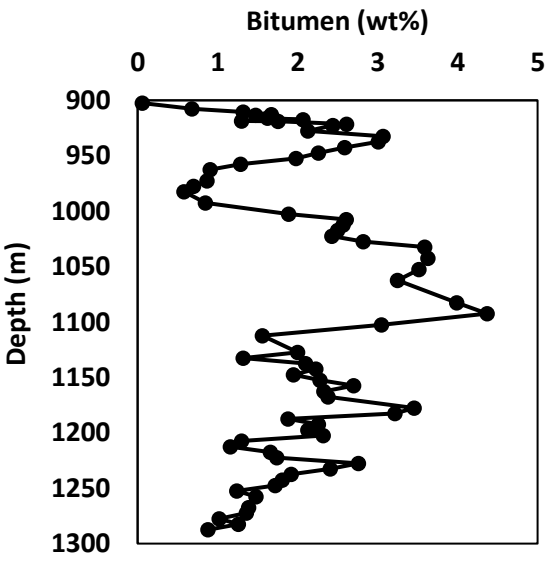

Fig. 5: Bitumen (wt%) with depth for the NESS 2 well as determined by Soxhlet extraction.

χ_w using NMR core data

We consider the components used for the connectivity theory-based resistivity model in the immature and early-stage mature cases. In the immature stage, the organic-rich chalk contains mostly calcite, immature kerogen, and water in both the macropores and micropores. During early-stage maturation, the kerogen generates bitumen and lighter hydrocarbons. Once bitumen is expelled into the macropores, some of the macropore space becomes oil wet.. We assume that the micropores remain water-wet and contain only water as demonstrated by D_2O diffusion eliminating the entire H_2O signal from the micropores The macropore system is mixed-wet, and for the purposes of our model, we assume that the water is in water-wet macropores, while the light hydrocarbons are in oil-wet pores. Our electrical resistivity model therefore has three classes of pores: water-wet micritic pores, water-wet macropores, and oil-wet macropores.

One method of estimating the values of χ_w is by using NMR T_2 distributions for "as received" core and fully saturated with brine. Downhole, the light hydrocarbons (NGLs) are in the oil-wet pores but the NGLs blow out of the core on the trip to the surface. This provides a method for separating the volume of water-wet and oil-wet macropores.

The laboratory NMR analysis was performed at Rice University as detailed in Chen et al. [2]. An Oxford Instruments GeoSpec2 rock-core analyzer was used with a Larmor frequency of 2.3 MHz to match that of the MREX logging tool.

Fig. 6 shows the T_2 distribution of an early-stage mature Ghareb sample from 920m in the NESS 2 well [2,11]. The region with the shortest T2 values, depicted in the A region of the spectrum (3 ms and shorter), responds to part of the bitumen. Kerogen has relaxation times which are too short to be detected by this NMR spectrometer. Bitumen also has values which are short, but a fraction may be detected if the viscosity is low enough. Region B, which includes T_2 values between 3 and 32 ms, is the response due to the water-wet micritic calcite. The signal with the longer relaxation time in region C (T_2 greater than 32 ms) responds to the fluids in the macro pore space. The separation of the T2 distribution for water into regions B and C, corresponding to the micritic and macropores, is a result of weak diffusive coupling due to bitumen blocking [11]. The water molecules no longer diffuse easily between the two spaces because bitumen is blocking many of the pore throats. Downhole, region C contains some connate water in the macropore space as well as methane and condensates.

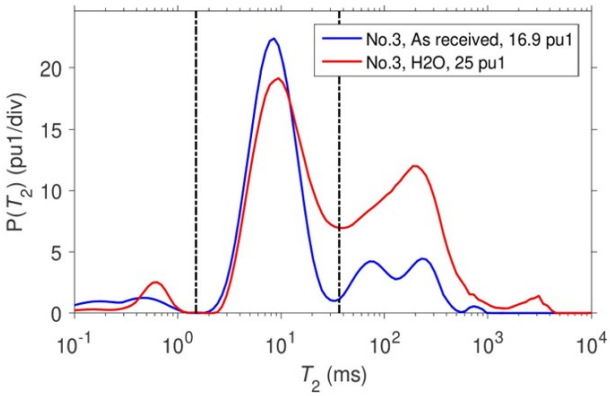

Fig. 6: NMR T_2 distribution of a core sample from the NESS 2 well at 920m, "as received" and after saturating with brine [2,11].

The light hydrocarbons in this core is taken to be the difference between the porosity in the "as received" core and the porosity when fully brine saturated. The micritic porosity is about 12 pu and the macro porosity of the as received core is about 4.9 pu. When saturated with brine, the macro porosity is 13 pu. The oil-wet macro porosity is taken to be the difference between the brine-saturated total porosity and the "as received" total porosity, or 8.1 pu. The fraction of the oil-wet macropore space is 8.1pu/13pu = 0.62. The bulk volume micritic portion of the rock is 25%, which implies that the porosity of the micritic portion is 48%. S_{co} is about 0.65 [6]. Using $\mu_m = 1.5$ and $\mu = 2$, the value of χ_w is about 0.028. This value agrees with the 0.03 fit to the resistivity index dataset in **Fig. 1**.

χ_w measured from core

The electrical resistivity profile of the organic-rich chalk at these maturity levels shows a significant increase compared to the immature case-more than would be expected for an Archie-type rock because of curvature. **Table 1** shows the Dean-Stark core data for a set of samples from the NESS 5 well in the Golan basin. **Fig. 7a** shows the fit of the Dean-Stark core data to the Archie resistivity model. The fit for the Archie model is best when m=4 and n=3.5; however, the brine resistivity is very low: 0.03 ohm-m. **Fig. 7b** shows the fit of the Dean-Stark core data to the connectivity theory-based resistivity model. The fit when χ_w=0.03 and μ=2 gives a brine resistivity of 1.2 ohm-m, which is the measured brine resistivity in the Upper Ghareb. **Fig. 8** shows the excellent fit between the electrical resistivity using the connectivity theory-based model ($\chi_w = 0.03, \mu = 2,\ R_w = 1.2$ ohm-m) with the Dean Stark core data shown in **Table 1** versus the NESS 5 resistivity well log in the Golan basin.

Table 1: Dean-Stark core data and resistivity log values for the NESS 5 well from 1050-1056m

Depth (m)	Phi	S_w	Rt (Ω-m)
1050.7	0.13	0.16	8370
1050.9	0.12	0.31	13544
1051.2	0.14	0.35	7510
1051.4	0.15	0.31	5545
1051.8	0.13	0.38	2935
1052.1	0.14	0.38	2023
1052.4	0.17	0.35	2023
1052.7	0.16	0.47	787
1052.8	0.17	0.53	473
1054.4	0.18	0.69	79
1054.8	0.20	0.73	103
1055.2	0.18	0.75	140
1055.4	0.18	0.70	167
1055.7	0.16	0.69	137
1055.9	0.15	0.66	129

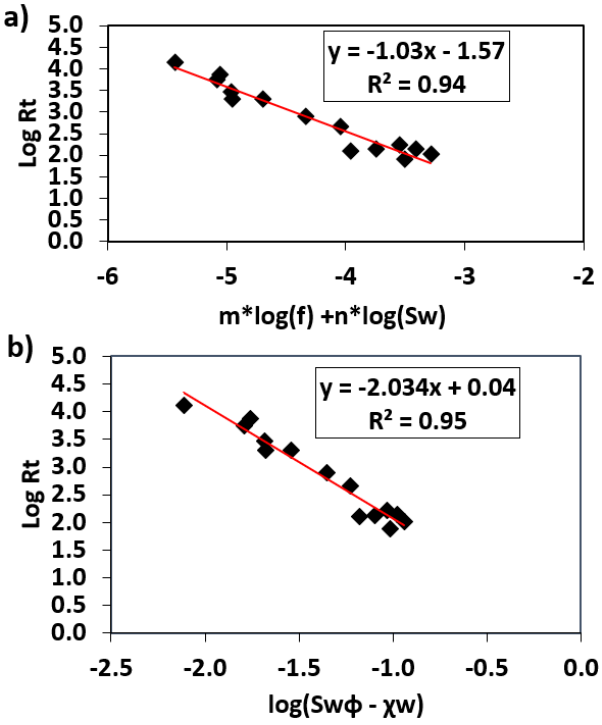

Fig. 7: a) Regression to fit Archie parameters for the NESS 5 well from 1050-1056m. m=4 and n=3.5 fit this dataset, but R_w is only 0.03 ohm-m. **b)** Regression to fit connectivity theory parameters for the NESS 5 well from 1050-1056m. $\chi_w = 0.03$ and $\mu = 2$ gives R_w=1.2 ohm-m.

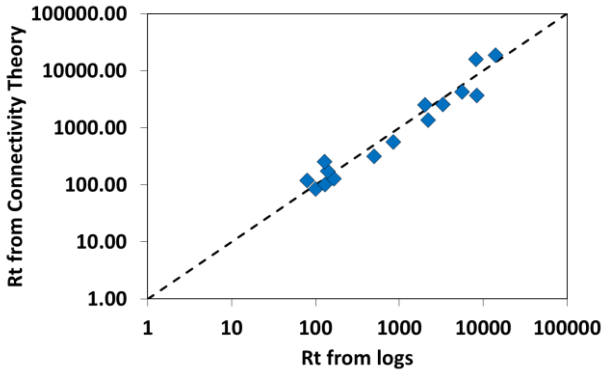

Fig. 8: Resistivity from NESS 5 well log from 1050-1056m versus resistivity calculated using the connectivity theory model, with $\chi_w = 0.03$ and $\mu = 2$.

Comparison between dielectric and resistivity log using connectivity theory

The $S_w\phi$ term in the connectivity theory-based resistivity model (Eq. 3) is directly measured with the dielectric log. One advantage of using the dielectric log in this model is that it is not necessary to use two separate logs to determine ϕ and S_w independently.

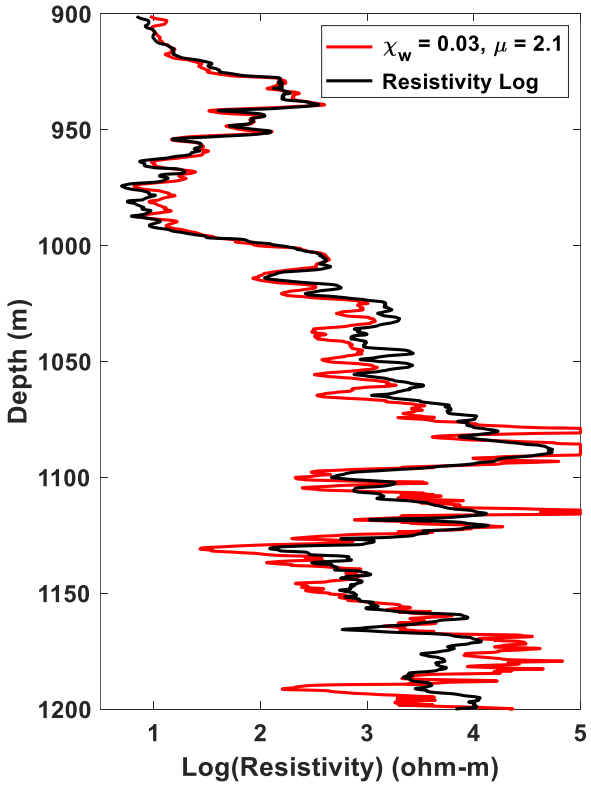

Fig. 9: Resistivity log from the NESS 2 well overlaid with the connectivity theory resistivity calculated from Eq. 3 using the dielectric log for $S_w\phi$, $\chi_w = 0.03$, and $\mu = 2.1$.

The NESS 2 resistivity log was overlaid with the connectivity model (Eq. 3) using the dielectric log for ϕS_w, $\chi_w = 0.03$, and $\mu = 2.1$ in **Fig. 9**. The brine resistivity R_w is 0.3 ohm-m which matches the R_w using Archie's equation in the organic-free carbonate at the top of the Ghareb. We note there is excellent agreement for over 300 meters of organic-rich rock with resistivity values ranging from less than 10 to over 10,000 ohm-m and porosities from 10 to 35 pu.

Conclusions

1. The amount of bitumen in macropores increases with organic maturity, creating a mixed-wet pore system with water-wet micritic pores and some oil-wet and some water-wet macropores.

2. The change in wettability causes a curvature in the I-S_w relation, resulting in a non-Archie behavior. NMR measurements on core show the micritic pores remain water-wet even at high bitumen content.

3. Comparing immature and post-pyrolysis resistivity, the change to non-Archie behavior occurs at T_{max} ~ 420°C, where the bitumen content increases rapidly. A connectivity model using $\mu = 2$ and $\chi_w = 0.03$ matches the post-pyrolysis data.

4. Dean Stark core data in NESS 5 shows the connectivity theory-based resistivity model provides a good fit to the I-S_w curvature with the same value of connectivity parameter ($\chi_w = 0.03$).

5. The value of χ_w can be explained using NMR T_2 relaxation data on "as received" and fully brine-saturated core.

6. Comparing the resistivity and dielectric logs in NESS 2, and using the value of $\chi_w = 0.03$ previously measured, we obtain an excellent match over a large calcareous section of ~300 m, covering an extremely wide range in resistivity and porosity.

Acknowledgements

We thank Weidong Li and Mohammad Chohan from Baker Hughes, Professor George Hirasaki, Professor Philip Singer, Zeliang Chen, and Xinglin Wang from Rice University, and Itay Reznick from the Geological Survey of Israel for their contributions to this paper.

Symbols and Abbreviations

NMR = Nuclear Magnetic Resonance
R_t = electrical resistivity of the saturated rock
R_w = electrical resistivity of the brine
ϕ = porosity
S_w = brine saturation
m = cementation exponent
n = saturation exponent
P = probability that a site will be conductive
P_c = pseudo-percolation threshold
χ_w = water connectivity correction index
μ = conductivity exponent
μ_m = conductivity exponent of the micritic portion of the rock
x_m = bulk volume fraction of rock that contains micritic grains
ϕ_m = porosity of the micritic portion of the rock
x_o = fraction of macro pores that are oil-wet
S_{co} = critical oil saturation at which conductive fluids no longer percolate
ϕ_M = porosity of the macro pores
T_{max} = temperature of peak S2 response during programmed Rock-Eval pyrolysis
TOC = total organic carbon

References

1. R.L. Kleinberg, W.E. Kenyon, P.P. Mitra, Journal of Magnetic Resonance, Series A **108**, 206-214 (1994)
2. Z. Chen, P.M. Singer, X. Wang, H.J. Vinegar, S.V. Nguyen, G.J. Hirasaki, Petrophysics **60**, 771-797 (2019)
3. D. Kennedy, Petrophysics **48**, 335-361 (2007)
4. A.P. Garcia, Z. Heidari, A. Rostami, Petrophysics **58**, 454-469 (2017)
5. B. Montaron, *15th SPE Middle East Oil & Gas Show and Conference* (2007)
6. B. Montaron, Petrophysics **50**, 102-115 (2009)
7. G.E. Archie, *SPE 942054-G, Transactions, AIME* **146**, 54-62 (1942).
8. W.G. Anderson, *SPE 13932* (1986)
9. J. Birchak, L. Gardner, J. Hipp, J. Victor, *IEEE Proceedings* **62**, 93-98 (1974)
10. J.G. Berryman, *Mixture Theories for Rock Properties, Rock Physics and Phase Relations- A Handbook of Physical Constants*, 205-228 (1995)
11. E.G. Vinegar, Y.O. Rosenberg, I. Reznick, Y. Gordin, P.M. Singer, X. Wang, Z. Chen, S.V. Nguyen, W. Li, T. Bradley, G.J. Hirasaki, L.W. Lake, S. Feinstein, Y. H. Hatzor, H.J. Vinegar, *SPWLA 61st Annual Logging Symposium* (2020)
12. I. Kutuzov, M.Sc. Thesis. Ben-Gurion of the Negev, Be'er Sheva, Israel (2017)
13. Y. O. Rosenberg, I. J. Reznick, H. J. Vinegar, S. Feinstein, Y. Bartov, Marine and Petroleum Geology (2020)